

Exponential Tracking Control of a Hydraulic Proportional Directional Valve and Cylinder via Integrator Backstepping*

J. Chen¹, W. E. Dixon², J. R. Wagner¹, and D. M. Dawson¹

¹Departments of ECE and ME, Clemson University, Clemson, SC 29634-0915

²Engineering Science and Technology Division - Robotics, Oak Ridge National Laboratory,
P.O. Box 2008, Oak Ridge, TN 37831-6305

E-mail: dixonwe@ornl.gov, Telephone: (865) 574-9025

Keywords: Hydraulics, Nonlinear Control Application, Backstepping, And Exponential Stability

"The submitted manuscript has been authored by a contractor of the U.S. Government under contract No. DE-AC05-96OR22464. Accordingly, the U.S. Government retains a nonexclusive, royalty-free license to publish or reproduce the published form of this contribution, or allow others to do so, for U.S. Government purposes."

To appear at the ASME International Mechanical Engineering Congress and Expo,
Nov. 17-22, 2002, New Orleans, Louisiana

* This research was supported in part by the Eugene P. Wigner Fellowship Program of the Oak Ridge National Laboratory (ORNL), managed by UT-Battelle, LLC, for the U.S. Department of Energy (DOE) under contract DE-AC05-00OR22725 and in part by the U.S. DOE Environmental Management Sciences Program (EMSP) project ID No. 82797 at ORNL, and by U.S. NSF Grant DMI-9457967, ONR Grant N00014-99-1-0589, a DOC Grant, and an ARO Automotive Center Grant.

IMECE2002-32076

EXPONENTIAL TRACKING CONTROL OF A HYDRAULIC PROPORTIONAL DIRECTIONAL VALVE AND CYLINDER VIA INTEGRATOR BACKSTEPPING¹

J. Chen,[†] W. E. Dixon,[‡] J. R. Wagner,[§] and D. M. Dawson[†]

[†]Dept. of Electrical and Computer Engineering, Clemson University, Clemson, SC 29634-0921

[‡]Eng. Science and Tech. Div. - Robotics, Oak Ridge National Laboratory, Oak Ridge, TN 37831-6305

[§]Dept. of Mechanical Engineering, Clemson University, Clemson, SC 29634-0921

(864) 656-7376, email: jwagner@clemson.edu

ABSTRACT

Hydraulic systems are widely used in manufacturing processes and transportation systems where energy intensive operations are performed and “machine” control is vital. A variety of flow control products exist including manual directional control valves, proportional directional control valves, and servovalves. The selection of a control valve actuation strategy is dependent on the system response requirements, permissible pressure drop, and hardware cost. Although high bandwidth servovalves offer fast response times, the higher expense, susceptibility to debris, and pressure drop may be prohibitive. Thus, the question exists whether the economical proportional directional control valve’s performance can be sufficiently enhanced using nonlinear control strategies to begin approaching that of servovalves. In this paper, exponential tracking control of a hydraulic cylinder and proportional directional control valve, with spool position feedback, is achieved for precise positioning of a mechanical load. An analytical and empirical mathematical model is developed which describes the transient behavior of the integrated components. A nonlinear backstepping control algorithm is designed to accommodate inherent system nonlinearities.

1 INTRODUCTION

A wide range of industries that utilize hydraulic systems, such as off-road construction and agricultural equipment manufacturers, as well as the machine tool industry, are continually demanding decreased package sizes, finer system control, faster response, and multi-tasking systems without added expense. For example, forestry machines are required to navigate difficult terrain, cultivate timber, and prepare the soil for replanting under confined operating conditions (Papadopoulos, 1997). Farm implements such as combines, harvesters, and planters require nonlinear speed and position control of the power-take-off shaft as a result of time varying loads. Automated manufacturing systems use multi-axis rotating machining centers frequently located on shop floors where space is at a premium. Finally, aircraft control systems require responsive compact hydraulic systems to reliably position the landing gear, flaps, and rudders. Electrically actuated fluid valves afford engineers the opportunity to regulate hydraulic systems under computer control for enhanced operation and diagnostics. Two of the more common hydraulic actuation valves available are the servo-solenoid and the traditional two-stage flapper/nozzle servo-valve.

The servo-solenoid valve integrates a proportional solenoid assembly in direct contact with the main valve spool. The generated solenoid force is typically proportional to the armature current which is dependent on the supplied voltage. Once the proportional solenoid armature has moved through its approach zone, the force generated for a given current will be approximately constant. The desired spool position is obtained by balancing the proportional

¹THIS RESEARCH WAS SUPPORTED IN PART BY THE EUGENE P. WIGNER FELLOWSHIP PROGRAM OF THE OAK RIDGE NATIONAL LABORATORY (ORNL), MANAGED BY UT-BATTELLE, LLC, FOR THE U.S. DEPARTMENT OF ENERGY (DOE) UNDER CONTRACT DE-AC05-00OR22725 AND IN PART BY THE U.S. DOE ENVIRONMENTAL MANAGEMENT SCIENCES PROGRAM (EMSP) PROJECT ID NO. 82797 AT ORNL, AND BY U.S. NSF GRANT DMI-9457967, ONR GRANT N00014-99-1-0589, A DOC GRANT, AND AN ARO AUTOMOTIVE CENTER GRANT.

solenoid force against a calibrated opposing spring force. Spool position feedback is achieved with a linear variable displacement transducer (LVDT) in direct contact with the main spool. Valves of this category are sometimes referred to as “stroke” controlled solenoids (Tonyan, 1985). While servo-solenoid valves are smaller in size (i.e., one stage), the spool overlap or dead band is generally greater (although valves may be purchased with zero dead band). However, the servo-solenoid valve may be as much as three times less expensive to manufacture, is well suited for applications where fluid contamination is prevalent, and has very low pressure losses in comparison to a conventional servo-valve (Yeaple, 1990).

The two stage servo-valve utilizes a torque motor and “flapper” configuration where the flapper moves against one of two orifices. A pressure differential is created across the second stage’s main spool which results in the spool shifting to the desired position. Mechanical feedback is transmitted back through the flapper to the torque motor which permits the main spool-valve position to be adjusted. One advantage of the servo-valve is the small moving mass which results in a higher natural frequency and faster response time. The disadvantages of flapper type servo-valves include envelope size restrictions, manufacturing costs due to tight machining tolerances, low tolerance for fluid contamination, and high pressure losses. The two stage servo-valve disadvantages have motivated engineers to consider using the servo-solenoid valve in fluid power designs.

A variety of control architectures have been proposed and applied to regulate the operation of nonlinear hydraulic systems. The classical proportional-integral-derivative (PID) control technique generally results in poor tracking for higher frequency fluid applications. During the past decade, several high precision controllers have been designed which consider the underlying nonlinear system’s dynamics. Alleyne (1995) developed an adaptive sliding mode controller for use with active vehicle suspension systems. Bu (2000) developed a robust controller that considers parametric uncertainties while achieving asymptotic output tracking. Linear control theory was applied by Bobrow (1995) to design an adaptive hydraulic servo-valve controller using full-state feedback for simultaneous parameter identification and tracking control. Vossoughi (1995) created, and experimentally verified, a globally linearizing feedback control law for electrohydraulic systems which demonstrated uniform response across a wider range of operating conditions. Gamble (1994) presents a comparison of sliding mode control with state feedback and PID control for proportional solenoid valves. The sliding mode controller exhibited the best overall performance in terms of steady-state error, response time, overshoot, and symmetry.

Alleyne (1996) developed a Lyapunov-based control algorithm that compensates for parametric uncertainty in the dynamic model of a two-stage servo-valve undergoing force tracking. Plummer (1996) applied a self-tuning adaptive controller to an electrohydraulic positioning system with varying load stiffness and supply pressure. A nonlinear adaptive learning algorithm was proposed by Zheng (1998) for a proportional valve to accommodate valve dead zones, valve flow saturation, and cylinder seal friction. Sohl (1999) studied friction compensation using a Lyapunov function that provided exponentially stable force and position trajectory tracking. Adaptive robust controllers have been designed by Bu (1999) and Yao (2000) for electrohydraulic systems with parametric and nonlinearity uncertainties to track prescribed outputs. Recently, the nonlinear characteristics of proportional directional control valves have been studied by Bu (2000) without consideration of the valve dynamics for simplicity. Although the previous control strategies have successfully been applied to hydraulic systems, a new control strategy is designed and investigated in this paper as a means for performance improvements. That is, rather than utilizing a first order approximation as in many of the previous results (e.g., (Alleyne, 1996)), performance improvements are investigated by developing a control strategy based on an approximation of the nonlinear fluid flow dynamics. By developing a differentiable approximation of the nonlinear fluid flow dynamics, integrator backstepping techniques can be utilized to develop a controller for the full order system. Specifically, by using Lyapunov-based design and analysis techniques, exponential tracking of the hydraulic cylinder position is achieved.

This paper is organized as follows. In Section 2, behavioral models for the electrical, hydraulic, and mechanical system components are developed. Section 3 introduces the nonlinear controller design and analysis. Concluding remarks are presented in Section 4.

2 BEHAVIORAL MODELS

The behavioral models for the multiple domain electrohydraulic and mechanical system can be partitioned into three coupled subsystems: electrical (solenoid dynamics), hydraulic (spool valve dynamics), and mechanical (cylinder dynamics). Figures 1 and 2 illustrate an experimental system which corresponds to a general hydraulic system featuring integrated translational and rotational actuators; in this application, only the hydraulic cylinder shall be considered. The modeled portion of the system consists of a Bosch NG6 servo-solenoid control valve (e.g., nonlinear solenoid and main valve spool dynamics) and a Miller hydraulic cylinder with an attached mechanical load (Hardwick, 1984). To develop the underlying system dynamic descriptions, funda-

mental hydraulic, electrical, and mechanical concepts shall be applied.

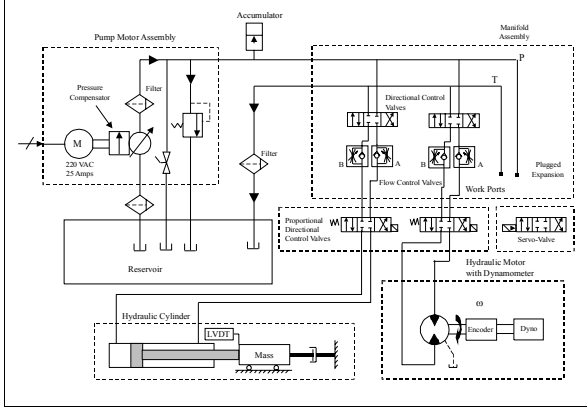


Figure 1. HYDRAULIC EXPERIMENTAL SYSTEM CONFIGURATION

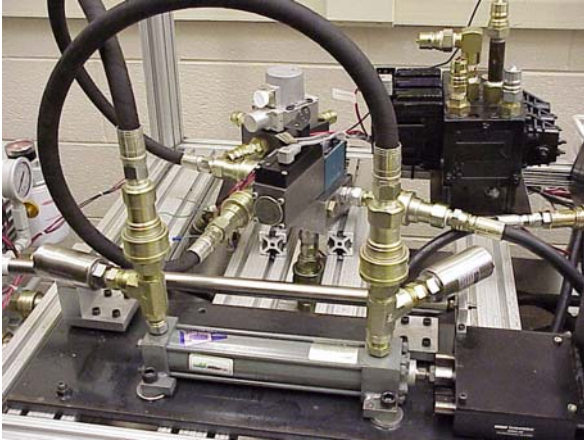


Figure 2. EXPERIMENTAL TEST CELL WITH A BOSCH NG6 SERVO SOLENOID VALVE AND SPOOL SENSOR

2.1 SOLENOID AND SPOOL DYNAMICS

The resistor-inductor circuit that electrically models the solenoid is given by the following expression

$$V_S = V_L + Ri \quad (1)$$

where $V_S(t) \in \mathbb{R}$ denotes the supply voltage, $V_L(t) \in \mathbb{R}$ denotes the voltage drop across the solenoid, $R \in \mathbb{R}$ denotes the armature resistance, and $i(t) \in \mathbb{R}$ denotes the measurable solenoid current. Motivated by the desire to relate the electrical dynamics given in (1) to the mechanical dynamics of the solenoid valve, the following relationship can be developed (Vaughan, 1996)

$$F_g = h(\lambda^2, z) \quad (2)$$

where $F_g(t) \in \mathbb{R}$ denotes the force generated by the solenoid, and $\lambda(t) \in \mathbb{R}$ denotes the solenoid flux linkage that can be related to $V_L(t)$ of (1) by using Faraday's Law as follows

$$\lambda = N \int \frac{d\Phi}{dt} dt = \int V_L dt \quad (3)$$

where $\Phi(t) \in \mathbb{R}$ denotes the magnetic flux and $N \in \mathbb{R}$ denotes the number of turns on the solenoid coil.

The expressions given in (1-3) relate the electrical dynamics to the force generated by the solenoid. Since the force generated by the solenoid acts on the main spool valve to control fluid flow within the attached hydraulic actuator, the force generated by the solenoid is also coupled to the electrical dynamics. Specifically, by applying Newton's law to the system shown in Figure 3, the spool valve dynamics can be related to $F_g(t)$ as follows (Vaughan, 1996)

$$\ddot{z} = \frac{1}{m_s} (-b_s \dot{z} - k_s z + F_g + F_{flow}) \quad (4)$$

where $z(t)$, $\dot{z}(t)$, $\ddot{z}(t) \in \mathbb{R}$ denote the spool position, velocity, and acceleration, respectively, the constant, known coefficients $k_s, b_s \in \mathbb{R}$ denote the spool return spring stiffness and the spool damping constant, respectively, $m_s \in \mathbb{R}$ denotes the spool mass, and $F_{flow}(t) \in \mathbb{R}$ denotes the flow force through a constriction (Wright, 1997). To facilitate the subsequent control development, the spool valve dynamics are rewritten in the following simplified form

$$\ddot{z} = \frac{1}{m_s} (u - N_s) \quad (5)$$

where $u(t) = F_g(t)$ denotes the subsequently designed control force applied by the solenoid to the spool, $N_s(z, \dot{z}) \in \mathbb{R}$ is the spring/damping term which may be expressed as follows

$$N_s = b_s \dot{z} + k_s z \quad (6)$$

and the constriction fluid flow force has been neglected for simplicity.

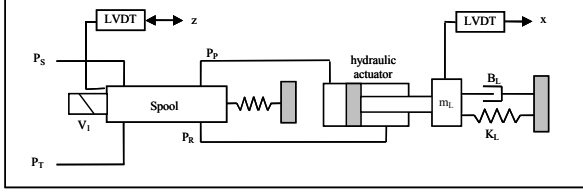


Figure 3. HYDRAULIC VALVE SPOOL AND CYLINDER ASSEMBLY FOR MODEL DEVELOPMENT

Remark 1. Due to the physical construction of the cylinder, the spool position is restricted to a certain region; hence, it is clear that $z(t) \in \mathcal{L}_\infty$.

Remark 2. As stated in Merritt (1967), the steady-state and transient contributions to the fluid flow force through a constriction may be defined as

$$F_{flow} = 2C_d w z (\Delta P) \cos \phi + C_d w l \sqrt{2\rho |\Delta P|} \dot{z} \quad (7)$$

$$+ \frac{C_d w l z}{\sqrt{(2/\rho) |\Delta P|}} \frac{d}{dt} (\Delta P)$$

where $\rho \in \mathbb{R}$ is the fluid density, $w \in \mathbb{R}$ denotes the area gradient of the orifice, $C_d \in \mathbb{R}$ is the discharge coefficient, $\phi \in \mathbb{R}$ is the flow angle, $l \in \mathbb{R}$ is the axial distance between the incoming and outgoing flow, and $\Delta P \in \mathbb{R}$ is the pressure difference across the constriction.

2.2 CYLINDER DYNAMICS

The governing equation for the hydraulic cylinder displacement must consider both the hydraulic and mechanical forces such that

$$\ddot{x} = \frac{1}{m_L} (P_P A_P - P_R A_R - b_L \dot{x} - k_L x - F_L) \quad (8)$$

where $x(t)$, $\dot{x}(t)$, $\ddot{x}(t) \in \mathbb{R}$ represent the position, velocity, and acceleration of the cylinder piston, respectively, $P_P(t)$, $P_R(t) \in \mathbb{R}$ are the respective piston and rod side cylinder pressures (acting on respective cylinder areas denoted by $A_P, A_R \in \mathbb{R}$), and $F_L \in \mathbb{R}$ denotes a constant externally applied load on the cylinder. The known, constant coefficients $b_L, k_L \in \mathbb{R}$ given in (8) represent damping and compliance

elements within the system (including damping and compliance effects by the load). To facilitate the subsequent control development, the cylinder dynamics are rewritten in the following simplified form

$$\ddot{x} = \frac{1}{m_L} (F - N) \quad (9)$$

where $N(x, \dot{x}) \in \mathbb{R}$ is the spring/damping forces given by the following expression

$$N = b_L \dot{x} + k_L x + F_L \quad (10)$$

$F(P_P, P_R) \in \mathbb{R}$ denotes the force applied by the hydraulic flow control valve and is defined as follows

$$F = P_P A_P - P_R A_R. \quad (11)$$

The piston and rod side cylinder pressures given in (8) and (11) are governed by the following differential expressions (Merritt, 1967)

$$\dot{P}_P = \frac{\beta_e}{A_P x} (Q_p - A_p \dot{x} - C_{ip}(P_P - P_R) - C_{ep} P_P) \quad (12)$$

$$\dot{P}_R = \frac{\beta_e}{A_R (L - x)} (-Q_R + A_R \dot{x} + C_{ip}(P_P - P_R) - C_{ep} P_R) \quad (13)$$

where $C_{ip}, C_{ep} \in \mathbb{R}$ denote known, constant, internal, and external leakage coefficients, respectively, and $\beta_e \in \mathbb{R}$ is the known effective bulk modulus. $L \in \mathbb{R}$ is the length of the cylinder. The fluid flow entering and exiting the cylinder given in (12) and (13), denoted by $Q_P(z, P_P)$, $Q_R(z, P_R) \in \mathbb{R}$, are derived from the application of flow continuity between the cylinder and the directional valve as follows (Merritt, 1967)

$$Q_P = k_P z \sqrt{\Delta P_P}, \quad \Delta P_P = \begin{cases} P_S - P_P & \text{for } z \geq 0 \\ P_P - P_T & \text{for } z < 0 \end{cases} \quad (14)$$

$$Q_R = k_R z \sqrt{\Delta P_R}, \quad \Delta P_R = \begin{cases} P_R - P_T & \text{for } z \geq 0 \\ P_S - P_R & \text{for } z < 0 \end{cases} \quad (15)$$

where $P_S, P_T \in \mathbb{R}$ represent the respective supply and tank pressures.

Remark 3. *The hydraulic cylinder is assumed to be constructed such that some volume always remains in the rod and piston sides of the cylinder due to the presence of a small amount of residual fluid that prevents the complete retraction or extension of the piston. Based on this assumption, it is clear that the following inequalities hold*

$$\delta_1 < x < \delta_2, \forall \delta_1 > 0, \delta_2 < L \quad (16)$$

and hence, potential singularities in the fluid dynamics given in (12) and (13) due to zero chamber volume are avoided.

The discontinuous nature of the nonlinear fluid flow dynamics given in (12-15) have inhibited the ability of previous control designs to address the full order model given by (9-15). For example, the discontinuous structure of (12-15) restricts the use of design tools such as integrator backstepping. To address this issue, researchers typically approximate the fluid dynamics by a first order system, potentially limiting the performance of the control structure. Motivated by the desire to address the full order dynamics as a means for improved performance, we develop a differentiable approximation for the dynamics given in (12-15) as follows

$$\dot{P}_P = \frac{\beta_e}{A_p x} (k_P f_{sP} z + N_P) \quad (17)$$

$$\dot{P}_R = \frac{\beta_e}{A_R (L - x)} (-k_R f_{sR} z + N_R) \quad (18)$$

where the fluid flow variables $f_{sP}(P_P, z), f_{sR}(P_R, z) \in \mathbb{R}$ approximate the variables $Q_P(z, P_P)$ and $Q_R(z, P_R)$ of (14) and (15) as follows

$$f_{sP} = \beta_0 + \frac{\beta_1 e^{\gamma z} - 1}{e^{\gamma z} + 1} \quad (19)$$

$$f_{sR} = \beta_2 + \frac{\beta_3 e^{-\gamma z} - 1}{e^{-\gamma z} + 1} \quad (20)$$

and $N_P(\dot{x}, P_P, P_R), N_R(\dot{x}, P_P, P_R) \in \mathbb{R}$ are defined as

$$N_P = -A_P \dot{x} - C_{ip}(P_P - P_R) - C_{ep} P_P \quad (21)$$

$$N_R = A_R \dot{x} + C_{ip}(P_P - P_R) - C_{ep} P_R. \quad (22)$$

The coefficients $\beta_0(P_P), \beta_1(P_P), \beta_2(P_R), \beta_3(P_R) \in \mathbb{R}$ given in (19) and (20) are defined as follows

$$\beta_0 = 1 + \sqrt{P_P - P_T} \quad (23)$$

$$\beta_1 = \sqrt{P_S - P_P} - \sqrt{P_P - P_T} - 1 \quad (24)$$

$$\beta_2 = 1 + \sqrt{P_R - P_T} \quad (25)$$

$$\beta_3 = \sqrt{P_S - P_R} - \sqrt{P_R - P_T} - 1 \quad (26)$$

where the supply and tank pressures are assumed to satisfy the following inequalities

$$P_S > \max(P_P, P_R), \quad P_T < \min(P_P, P_R) \quad (27)$$

and $\gamma \in \mathbb{R}$ denotes a constant, known modeling coefficient. Figure 4 illustrates that (19) and (20) provide a differentiable approximation of the discontinuous terms $\sqrt{\Delta P_P}$ and $\sqrt{\Delta P_R}$ of (14) and (15), respectively. In Figure 4, $\sqrt{\Delta P_P}, \sqrt{\Delta P_R}, f_{sP}(P_P, z)$, and $f_{sR}(P_R, z)$ are plotted with $P_P(t)$ and $P_R(t)$ held constant while $z(t)$ is varied with the modeling parameter $\gamma = 1000$.

CONTROLLER DESIGN

The control objective in this paper is to force the piston position of a hydraulic cylinder to track a time varying reference trajectory. To quantify the control objective, the piston tracking error $e(t) \in \mathbb{R}$ is defined as

$$e = x_d - x \quad (28)$$

where $x_d(t) \in \mathbb{R}$ and its first five time derivatives are assumed to be bounded. To facilitate the controller design and stability analysis, a filtered tracking error, denoted by $r(t) \in \mathbb{R}$, is defined as

$$r = \dot{e} + \alpha e. \quad (29)$$

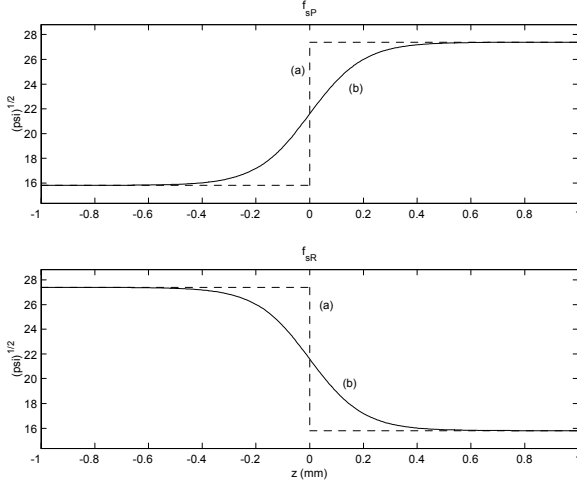


Figure 4. APPROXIMATION OF $\sqrt{P_p(z)}$, $\sqrt{P_r(z)}$ (DENOTED BY (a)) BY $f_{sp}(\cdot)$ AND $f_{sr}(\cdot)$ (DENOTED BY (b)), RESPECTIVELY.

As indicated in the model development given in Section 2, the solenoid control force $u(t)$ is indirectly related to the cylinder piston position through the spool dynamics; hence, as a means to relate $u(t)$ to the cylinder piston position, the subsequent control design is based on the integrator backstepping approach. Specifically, from (9) it is evident that the position of the cylinder piston is related to the control valve force $F(t)$. Since the control valve force cannot be directly actuated, the subsequent control design will first target the development of a desired control valve force, denoted by $F_d(t) \in \mathbb{R}$, and then target eliminating the mismatch between the actual and desired control value forces. To quantify the mismatch between the actual and desired control value forces, a force tracking error signal $\eta_f(t) \in \mathbb{R}$ is defined as

$$\eta_f = F_d - F. \quad (30)$$

By backstepping on the force tracking error signal, the time derivative of the desired control valve force can be related to a function of the spool position. Motivated by the desire to mitigate the force tracking error given in (30), a desired spool position function, denoted by $f_d(t) \in \mathbb{R}$, can then be designed, where the mismatch between the actual and desired spool position functions is quantified through a spool tracking error-like signal $\eta_z(t) \in \mathbb{R}$ defined as

$$\eta_z = f_d - \beta_e gz \quad (31)$$

where $z(t)$ and β_e are given in (4), (12), and (13), and

$g(x, z, P_P, P_R) \in \mathbb{R}$ is defined as follows

$$g = \frac{k_P f_{sP}}{x} + \frac{k_R f_{sR}}{L - x} \quad (32)$$

where $f_{sP}(\cdot)$, $f_{sR}(\cdot)$ are defined in (19) and (20), respectively. After backstepping on $\eta_z(t)$, the time derivative of the desired spool function can be related to the spool velocity. Motivated by the desire to mitigate the tracking error given in (31), a desired spool velocity, denoted by $\dot{z}_d(t) \in \mathbb{R}$, can then be designed, where the mismatch between the actual and desired spool velocities is quantified through a spool velocity tracking error $\eta_1(t) \in \mathbb{R}$ defined as follows

$$\eta_1 = \dot{z}_d - \dot{z}. \quad (33)$$

After backstepping on the spool velocity tracking error, the time derivative of the desired spool velocity can be related to the solenoid control force through (5); hence, $u(t)$ can then be designed to mitigate the backstepping error signals and to achieve the control objective. In the following sections, the error system development for $r(t)$, $\eta_f(t)$, $\eta_z(t)$, and $\eta_1(t)$ is provided along with the control designs for $F_d(t)$, $f_d(t)$, $\dot{z}_d(t)$, and $u(t)$.

2.3 CONTROL DEVELOPMENT

To develop the open-loop error system for $r(t)$, we take the time derivative of (29) and multiply the resulting expression by m_L as follows

$$m_L \dot{r} = m_L (\ddot{x}_d + \alpha \dot{e}) - F_d + \eta_f + N \quad (34)$$

where (9), (28), and (30) were utilized. Based on the open-loop error system given in (34) and the subsequent stability analysis, the desired control valve force is designed as follows

$$F_d = m_L (\ddot{x}_d + \alpha \dot{e}) + N + k_1 r. \quad (35)$$

After substituting (35) into (34) for $F_d(t)$ and cancelling common terms, the following closed-loop error system for $r(t)$ can be obtained

$$m_L \dot{r} = \eta_f - k_1 r. \quad (36)$$

After taking the time derivative of (30) and utilizing (31), the following open-loop error system for $\eta_f(t)$ can be

obtained

$$\dot{\eta}_f = \dot{F}_d - \beta_e \left(\frac{N_P}{x} - \frac{N_R}{L-x} \right) - f_d + \eta_z \quad (37)$$

where we utilized the fact that the time derivative of the control valve force can be expressed as follows

$$\dot{F} = \beta_e \left(\frac{N_P}{x} - \frac{N_R}{L-x} + gz \right) \quad (38)$$

where $z(t)$ and $g(\cdot)$ are defined in (5) and (32), respectively. Based on the structure of (37) and the subsequent stability analysis, $f_d(t)$ is designed as follows

$$f_d = \dot{F}_d - \beta_e \left(\frac{N_P}{x} - \frac{N_R}{L-x} \right) + k_2 \eta_f + r \quad (39)$$

where $\dot{F}_d(t)$ can be determined by taking the time derivative of (35) and utilizing (9), (10), (28), and (29) as follows

$$\begin{aligned} \dot{F}_d = m_L \left(x_d^{(3)} + \alpha \ddot{x}_d \right) + \left(\frac{b_L}{m_L} - \alpha \right) (F - N) \\ + k_L \dot{x} + \frac{k_1}{m_L} (\eta_f - k_1 r). \end{aligned} \quad (40)$$

After substituting (39) into (37) for $f_d(t)$ and canceling common terms, the following closed-loop error system for $\eta_f(t)$ can be obtained

$$\dot{\eta}_f = \eta_z - k_2 \eta_f - r. \quad (41)$$

After taking the time derivative of (31), the following open-loop error system for $\eta_z(t)$ can be obtained

$$\dot{\eta}_z = \dot{f}_d - \beta_e (g\dot{z} + \dot{g}z) \quad (42)$$

where

$$\dot{g} = (\nabla_x g) \dot{x} + (\nabla_z g) \dot{z} + (\nabla_{P_P} g) \dot{P}_P + (\nabla_{P_R} g) \dot{P}_R \quad (43)$$

where the notation $\nabla_x y(\cdot)$ denotes the partial derivative of $y(\cdot)$ with respect to x . The partial derivatives $\nabla_x g(x, z, P_P, P_R)$, $\nabla_z g(x, z, P_P, P_R)$, $\nabla_{P_P} g(x, z, P_P)$, $\nabla_{P_R} g(x, z, P_R) \in \mathbb{R}$ given in (43) can be determined as follows

$$\nabla_x g = \frac{k_R f_{sR}}{(L-x)^2} - \frac{k_P f_{sP}}{x^2} \quad (44)$$

$$\nabla_z g = \frac{k_P \gamma e^{\gamma z} (\beta_1 + 1)}{x (e^{\gamma z} + 1)^2} - \frac{k_R \gamma e^{-\gamma z} (\beta_3 + 1)}{(L-x) (e^{-\gamma z} + 1)^2} \quad (45)$$

$$\nabla_{P_P} g = \frac{k_P}{2x (e^{\gamma z} + 1)} \left(\frac{1}{\sqrt{P_P - P_T}} - \frac{e^{\gamma z}}{\sqrt{P_S - P_P}} \right) \quad (46)$$

$$\nabla_{P_R} g = \frac{k_R}{2(L-x) (e^{-\gamma z} + 1)} \left(\frac{1}{\sqrt{P_R - P_T}} - \frac{e^{-\gamma z}}{\sqrt{P_S - P_R}} \right). \quad (47)$$

After utilizing (33), the open-loop error system given in (42) can be rewritten as follows

$$\dot{\eta}_z = \dot{f}_d - \beta_e (z\xi + \zeta \dot{z}_d - \zeta \eta_1) \quad (48)$$

where $\zeta(x, z, P_P, P_R)$, $\xi(z, x, P_P, P_R, \dot{x}, \dot{P}_P, \dot{P}_R) \in \mathbb{R}$ are defined as follows

$$\zeta = (\nabla_z g) z + g \quad (49)$$

$$\xi = (\nabla_x g) \dot{x} + (\nabla_{P_P} g) \dot{P}_P + (\nabla_{P_R} g) \dot{P}_R. \quad (50)$$

Based upon the structure of (48) and the subsequent stability analysis, the desired spool velocity is designed as follows

$$\dot{z}_d = \frac{1}{\beta_e \zeta} \left(\dot{f}_d - \beta_e z \xi + k_3 \eta_z + \eta_f \right) \quad (51)$$

where $\dot{f}_d(t)$ is given by the following expression

$$\begin{aligned} \dot{f}_d = \ddot{F}_d - \beta_e \left(-\frac{N_P}{x^2} - \frac{N_R}{(L-x)^2} \right) \dot{x} \\ + \frac{\beta_e}{m_L} \left(\frac{A_P}{x} + \frac{A_R}{L-x} \right) (F - N) \\ + \beta_e \left(\frac{C_{ip} + C_{ep}}{x} + \frac{C_{ip}}{L-x} \right) \dot{P}_P \\ - \beta_e \left(\frac{C_{ip}}{x} + \frac{C_{ip} + C_{ep}}{L-x} \right) \dot{P}_R \\ + k_2 (\eta_z - k_2 \eta_f - r) + \frac{1}{m_L} (\eta_f - k_1 r) \end{aligned} \quad (52)$$

where $\ddot{F}_d(t)$ can be determined as follows

$$\begin{aligned} \ddot{F}_d &= m_L \left(x_d^{(4)} + \alpha x_d^{(3)} \right) \\ &+ \left(\frac{b_L}{m_L} - \alpha \right) \left(\beta_e \left(\frac{N_P}{x} - \frac{N_R}{L-x} + gz \right) - k_L \dot{x} \right) \\ &+ \frac{1}{m_L} \left(k_L - b_L \left(\frac{b_L}{m_L} - \alpha \right) \right) (F - N) \\ &+ \frac{k_1}{m_L} \left(\eta_z - k_2 \eta_f - r - \frac{k_1}{m_L} (\eta_f - k_1 r) \right). \end{aligned} \quad (53)$$

After substituting (51) into (48) for $\dot{z}_d(t)$, and canceling common terms, the following closed-loop error system for $\eta_z(t)$ can be obtained

$$\dot{\eta}_z = \beta_e \zeta \eta_1 - k_3 \eta_z - \eta_f. \quad (54)$$

After taking the time derivative of (33) and making use of (5), the open loop dynamics for $\eta_1(t)$ can be determined as follows

$$\dot{\eta}_1 = \ddot{z}_d - \frac{1}{m_s} (u - N_s). \quad (55)$$

Based upon the open-loop tracking error system given by (55) and the subsequent stability analysis, the control input $u(t)$ is designed as follows

$$u = m_s (\ddot{z}_d + \beta_e \zeta \eta_z + k_4 \eta_1) + N_s \quad (56)$$

where $\ddot{z}_d(t)$ denotes the time derivative of the desired spool velocity given in (51) (see the appendix for an explicit expression). After substituting (56) into (55) for $u(t)$ and canceling common terms, the closed-loop error system for $\eta_1(t)$ can be determined as follows

$$\dot{\eta}_1 = -\beta_e \zeta \eta_z - k_4 \eta_1. \quad (57)$$

2.4 STABILITY ANALYSIS

Theorem 1. *The backstepping controller given in (35), (39), (51), and (56) ensures exponential cylinder piston position tracking in the sense that*

$$|e(t)| \leq \lambda_0 |e(0)| \exp(-\lambda \min(k_1, k_2, k_3, k_4) t) \quad (58)$$

provided that the following sufficient condition is satisfied

$$|z(t)| \leq \frac{1}{\gamma} \quad (59)$$

where $\lambda_0, \lambda \in \mathbb{R}$ are some positive constants and γ is given in (19) and (20).

Proof: To prove (58), we define a nonnegative function $V(t) \in \mathbb{R}$ as follows

$$V = \frac{1}{2} m_L r^2 + \frac{1}{2} \eta_f^2 + \frac{1}{2} \eta_z^2 + \frac{1}{2} \eta_1^2 \quad (60)$$

where $V(t)$ can be lower and upper bounded as in the following inequalities

$$\lambda_1 \|\Psi\|^2 \leq V \leq \lambda_2 \|\Psi\|^2 \quad (61)$$

where $\lambda_1, \lambda_2 \in \mathbb{R}$ are positive bounding constants and $\Psi(t) \in \mathbb{R}^4$ is defined as follows

$$\Psi = [r \ \eta_f \ \eta_z \ \eta_1]^T. \quad (62)$$

After taking the time derivative of (60), substituting for the closed-loop error systems given in (36), (41), (48), and (57), and cancelling common terms, the following expression can be obtained

$$\dot{V} \leq -\min(k_1, k_2, k_3, k_4) \|\Psi\|^2 \quad (63)$$

where (62) was utilized. After utilizing (61), the expression given in (63) can be rewritten as follows

$$\dot{V} \leq -\frac{1}{\lambda_2} \min(k_1, k_2, k_3, k_4) V. \quad (64)$$

Standard arguments can now be invoked to solve the differential inequality given in (64) as follows

$$V(t) \leq V(0) \exp\left(-\frac{1}{\lambda_2} \min(k_1, k_2, k_3, k_4) t\right). \quad (65)$$

Based on (61) and (65), the following inequality can now be developed

$$\|\Psi(t)\| \leq \|\Psi(0)\| \sqrt{\frac{\lambda_2}{\lambda_1} \exp\left(-\frac{1}{\lambda_2} \min(k_1, k_2, k_3, k_4) t\right)} \quad (66)$$

where $\Psi(t)$ was defined in (62).

Based on (62), (66), and the previous development, we can now prove that all of the control signals are bounded. Specifically, from (62) and (66) it

is clear that $r(t), \eta_f(t), \eta_z(t), \eta_l(t) \in \mathcal{L}_\infty$. Given that $r(t), \eta_f(t), \eta_z(t) \in \mathcal{L}_\infty$, we can use (36) and (41) to prove that $\dot{r}(t), \dot{\eta}_f(t) \in \mathcal{L}_\infty$. Standard techniques can now be used along with (29), (28), and the fact $r(t), \dot{r}(t) \in \mathcal{L}_\infty$ to prove that $e(t), \dot{e}(t), \ddot{e}(t) \in \mathcal{L}_\infty$. Based on the fact that $e(t), \dot{e}(t), \ddot{e}(t) \in \mathcal{L}_\infty$ and the assumption that $x_d(t), \dot{x}_d(t), \ddot{x}_d(t), x_d^{(3)}(t), x_d^{(4)}(t), x_d^{(5)}(t) \in \mathcal{L}_\infty$, (28) can be used to prove that $x(t), \dot{x}(t), \ddot{x}(t) \in \mathcal{L}_\infty$. From (10) and the fact that $x(t), \dot{x}(t), \ddot{x}(t) \in \mathcal{L}_\infty$, we can now prove that $N(\cdot), \dot{N}(\cdot) \in \mathcal{L}_\infty$. Given that $r(t), \dot{e}(t), \ddot{x}(t), N(\cdot) \in \mathcal{L}_\infty$, (9) and (35) can now be used to prove that $F(\cdot), F_d(t) \in \mathcal{L}_\infty$. From the assumption given in (27) where P_S, P_T are known positive constants, we can conclude a priori that $P_P(\cdot), P_R(\cdot) \in \mathcal{L}_\infty$. Based on the fact that $P_P(\cdot), P_R(\cdot) \in \mathcal{L}_\infty$, we can use (23-26) to prove that $\beta_0(P_P), \beta_1(P_P), \beta_2(P_R), \beta_3(P_R) \in \mathcal{L}_\infty$. From the previous boundedness statements and the assumption that $z(t) \in \mathcal{L}_\infty$, we can use (19) and (20) to prove that $f_{sP}(\cdot), f_{sR}(\cdot) \in \mathcal{L}_\infty$. Based on the fact that $f_{sR}(\cdot) \in \mathcal{L}_\infty$, we can utilize (32) to prove that $g(\cdot) \in \mathcal{L}_\infty$. Given that $\dot{x}(t), P_P(\cdot), P_R(\cdot) \in \mathcal{L}_\infty$, (21) and (22) can be used to prove that $N_P(\cdot), N_R(\cdot) \in \mathcal{L}_\infty$. Based on the fact that $F(\cdot), N(\cdot), \dot{x}(t), \eta_f(t), r(t) \in \mathcal{L}_\infty$, (40) can be utilized to prove that $\dot{F}_d(t) \in \mathcal{L}_\infty$; hence, from (39) we can now prove that $f_d(t) \in \mathcal{L}_\infty$. After taking the time derivative of (30) and utilizing the facts that $\dot{\eta}_f(t), \dot{F}_d(t) \in \mathcal{L}_\infty$, it is straightforward that $\dot{F}(\cdot) \in \mathcal{L}_\infty$. Because $N_P(\cdot), N_R(\cdot), f_{sP}(\cdot), f_{sR}(\cdot), z(t) \in \mathcal{L}_\infty$, (17) and (18) can be utilized to prove that $\dot{P}_P(\cdot), \dot{P}_R(\cdot) \in \mathcal{L}_\infty$. Given that the facts that $z(t), \beta_1(P_P), \beta_3(P_R), P_P(\cdot), P_R(\cdot) \in \mathcal{L}_\infty$ and the assumption given in (27), we can prove that $\nabla_z g(\cdot), \nabla_{P_P} g(\cdot), \nabla_{P_R} g(\cdot) \in \mathcal{L}_\infty$; hence, given that $g(\cdot), \dot{P}_P(\cdot), \dot{P}_R(\cdot) \in \mathcal{L}_\infty$, we can also conclude that $\zeta(\cdot), \xi(\cdot) \in \mathcal{L}_\infty$. After taking the time derivative of (23-26) and utilizing the facts that $\dot{P}_P(\cdot), \dot{P}_R(\cdot) \in \mathcal{L}_\infty$, it is clear that $\dot{\beta}_0(\cdot), \dot{\beta}_1(\cdot), \dot{\beta}_2(\cdot), \dot{\beta}_3(\cdot) \in \mathcal{L}_\infty$. By taking the time derivative of (21) and (22) and utilizing the facts that $\ddot{x}(t), \dot{P}_P(\cdot), \dot{P}_R(\cdot) \in \mathcal{L}_\infty$, we can also conclude that $\dot{N}_P(\cdot), \dot{N}_R(\cdot) \in \mathcal{L}_\infty$.

To facilitate further analysis, we utilize (19-26), (32), and (45) and performing some algebraic manipulation to obtain the following expression

$$\begin{aligned} \zeta = & \frac{k_P e^{\gamma z}}{x(e^{\gamma z} + 1)^2} (1 + \gamma z + e^{\gamma z}) \sqrt{P_S - P_P} & (67) \\ & + \frac{k_P e^{\gamma z}}{x(e^{\gamma z} + 1)^2} (1 - \gamma z + e^{-\gamma z}) \sqrt{P_P - P_T} \\ & + \frac{k_R e^{-\gamma z}}{(L-x)(e^{-\gamma z} + 1)^2} (1 - \gamma z + e^{-\gamma z}) \sqrt{P_S - P_R} \\ & + \frac{k_R e^{-\gamma z}}{(L-x)(e^{-\gamma z} + 1)^2} (1 + \gamma z + e^{\gamma z}) \sqrt{P_R - P_T}. \end{aligned}$$

Based on (27), it is clear from (67) that

$$\zeta > \varepsilon_1 \quad \text{if} \quad 1 \geq \gamma |z(t)| \quad (68)$$

where $\varepsilon_1 \in \mathbb{R}$ is some positive constant. Based on the previous boundedness arguments, we can now utilize (48), (51), (52), (53), and (68) to prove that $\dot{f}_d(t), \dot{F}_d(t), \dot{z}_d(t), \dot{\eta}_z(t) \in \mathcal{L}_\infty$. Given that $\dot{z}_d(t), \eta_l(t) \in \mathcal{L}_\infty$, we can utilize (33) to prove that $\dot{z}(t) \in \mathcal{L}_\infty$. Since $\nabla_z g(\cdot), \nabla_{P_P} g(\cdot), \nabla_{P_R} g(\cdot), \dot{z}(t), \dot{P}_P(\cdot), \dot{P}_R(\cdot) \in \mathcal{L}_\infty$, (43) can be utilized to prove that $\dot{g}(\cdot) \in \mathcal{L}_\infty$. After taking the time derivative of the expressions given in (19) and (20) as follows

$$\dot{f}_{sP} = \dot{\beta}_0 + \frac{e^{\gamma z} \left(\dot{\beta}_1 (e^{\gamma z} + 1) + (\beta_1 + 1) \gamma \dot{z} \right)}{(e^{\gamma z} + 1)^2} \quad (69)$$

$$\dot{f}_{sR} = \dot{\beta}_2 + \frac{e^{-\gamma z} \left(\dot{\beta}_3 (e^{-\gamma z} + 1) - (\beta_3 + 1) \gamma \dot{z} \right)}{(e^{-\gamma z} + 1)^2} \quad (70)$$

and utilizing the previous boundedness arguments, we can prove that $\dot{f}_{sP}(\cdot), \dot{f}_{sR}(\cdot) \in \mathcal{L}_\infty$. After taking the time derivative of (17) and (18) to obtain the following expressions

$$\begin{aligned} \ddot{P}_P = & \frac{\beta_e}{A_P x} \left(\dot{N}_P + k_P \dot{f}_{sP} z + k_P f_{sP} \dot{z} \right) & (71) \\ & - \frac{\beta_e \dot{x}}{A_P x^2} (N_P + k_P f_{sP} z) \end{aligned}$$

$$\begin{aligned} \ddot{P}_R = & \frac{\beta_e}{A_R (L-x)} \left(\dot{N}_R - k_R \dot{f}_{sR} z - k_R f_{sR} \dot{z} \right) & (72) \\ & + \frac{\beta_e \dot{x}}{A_R (L-x)^2} (N_R - k_R f_{sR} z), \end{aligned}$$

the facts that $\dot{x}(t), \dot{N}_P(\cdot), \dot{N}_R(\cdot), \dot{f}_{sP}(\cdot), \dot{f}_{sR}(\cdot), z(t), \dot{z}(t) \in \mathcal{L}_\infty$ can be used to prove that $\ddot{P}_P(\cdot), \ddot{P}_R(\cdot) \in \mathcal{L}_\infty$. Given the previous boundedness arguments and the development given in the appendix, we can now prove that $F_d^{(3)}(t), \dot{f}_d(t), \dot{\zeta}(\cdot), \dot{\xi}(\cdot), \text{and } \ddot{z}_d(t) \in \mathcal{L}_\infty$; hence, from (56) and (55), we can conclude that $\dot{\eta}_l(t), u(t) \in \mathcal{L}_\infty$. Based on the fact that the closed-loop system is bounded provided the sufficient condition given in (59) is satisfied, the result given in (58) can now be obtained from (66).

SUMMARY

The selection of a hydraulic flow control valve and accompanying actuation strategy is dependent on the system response requirements, permissible pressure drop, and hardware cost. Although high bandwidth servo-valves offer fast response times, the higher expense, susceptibility to debris, and pressure drop may be prohibitive. The performance of an economical proportional directional control valve, with spool position feedback, has been investigated in this paper using a nonlinear control strategy for the precise hydraulic cylinder positioning of a mechanical load. Analytical and empirical mathematical models were developed and experimentally validated to describe the transient behavior of the integrated components. An exponential tracking control algorithm with integrator backstepping was designed to accommodate inherent system nonlinearities. Future work will target testing the developed algorithm on an experimental testbed to demonstrate the performance of the nonlinear controller. Further research into servo-valves is warranted to fully explore the limitations of proportional directional control valves.

ACKNOWLEDGMENT

The authors wish to acknowledge the contributions of Mark Schubert for developing the behavioral models and a hydraulic test stand for future experimental testing.

REFERENCES

- Alleyne, A. and Hedrick, K. H., "Nonlinear Adaptive Control of Active Suspensions," *IEEE Transactions on Control Systems Technology*, Vol. 3, No. 1, pp. 94-101, 1995.
- Alleyne, A., "Nonlinear Force Control of an Electrohydraulic Actuator," Proceedings of the Japan-USA Symposium on Flexible Automation, Vol. 1, pp. 193-200, Boston, MA, 1996.
- Bobrow, J. E. and Lum, K., "Adaptive, High Bandwidth Control of a Hydraulic Actuator," Proceedings of the American Control Conference, Part 1 (of 6), pp. 71-75, Seattle, WA, 1995.
- Bu, F. and Yao, B., "Adaptive Robust Precision Motion Control of Single-Rod Hydraulic Actuators with Time-Varying Unknown Inertia: A Case Study," Proceedings of the ASME Dynamic Systems and Control Division, Vol. 6, pp. 131-138, Nashville, TN, 1999.
- Bu, F. and Yao, B., "Performance Improvement of Proportional Directional Control Valves: Methods and Experiments," Proceedings of the ASME Dynamic Systems and Control Division, Vol. 1, pp. 297-304, Orlando, FL, 2000.
- Bu, F. and Yao, B., "Nonlinear Adaptive Robust Control of Hydraulic Actuators Regulated by Proportional Directional Control Valves with Deadband and Nonlinear Flow Gain Coefficients," Proceedings of the American Control Conference, pp. 4129-4133, Chicago, IL, 2000.
- Dawson, D. M., Hu, J., and Burg, T. C., *Nonlinear Control of Electric Machinery*, Marcel Dekker, New York, 1998.
- Gamble, J. B. and Vaughan, N. D., "Comparison of Sliding Mode Control with State Feedback and PID Control Applied to a Proportional Solenoid Valve," Proceedings of the ASME Dynamic Systems and Control Division, Vol. 1, pp. 51-58, Chicago, IL, 1994.
- Hardwick, D. R., "Understanding Proportional Solenoids," *Hydraulics and Pneumatics*, Vol. 37, No. 8, pp. 58-60, 1984.
- Merritt, H. E., *Hydraulic Control Systems*, Wiley, New York, 1967.
- Papadopoulos, E., "Modeling and Identification of an Electrohydraulic Articulated Forestry Machine," Proceedings of the IEEE Conference on Robotics and Automation, Vol. 1, pp. 60-65, Albuquerque, NM, 1997.
- Plummer, A. R. and Vaughan, N. D., "Robust Adaptive Control for Hydraulic Servosystems," *Journal of Dynamic Systems, Measurement and Control*, Vol. 118, No. 2, pp. 237-244, 1996.
- Qian, W., Burton, R., Schoenau, G., and Ukrainetz, P., "A Comparison of a PID Controller to a Neural Net Controller in a Hydraulic System with Nonlinear Friction," Proceedings of the ASME Fluid Power Systems and Technology Group, Vol. 5, pp. 91-98, Anaheim, CA 1998.
- Sohl, G. A. and Bobrow, J. E., "Experiments and Simulations on the Nonlinear Control of a Hydraulic System," *IEEE Transactions on Control System Technology*, Vol. 7, No. 2, pp. 238-247, 1999.
- Tonyan, M. J., *Electronically Controlled Proportional Valves*, Marcel Dekker, New York, 1985.
- Vaughan, N. D. and Gamble, J. B., "The Modeling and Simulation of a Proportional Solenoid Valve," *Journal of Dynamic Systems, Measurement and Control*, Vol. 118, No. 1, pp. 120-131, 1996.
- Vossoughi, R. and Donath, M., "Dynamic Feedback Linearization for Electro-Hydraulically Actuated Control Systems," *Journal of Dynamic Systems, Measurement and Control*, Vol. 117, No. 4, pp. 468-477, 1995.
- Wright, H., Alleyne, A., and Liu, R., "On the Stability and Performance of Two-State Hydraulic Servovalves," Proceedings of the ASME Dynamic Systems and Control Division, Vol. 63, pp. 215-222, Dallas, TX, 1997.
- Yao, B., Fanping, B., Reedy, J., and Chiu, G., "Adaptive Robust Motion Control of Single-Rod Hydraulic Ac-

tuators: Theory and Experiments,” *IEEE/ASME Transactions on Mechatronics*, Vol. 5, No. 1, pp. 79-91, 2000.

Yeaple, M. J., *Fluid Power Design Handbook*, Marcel Dekker, New York, 1990.

Zheng, D., Havlicsek, H., and Alleyne, A., “Nonlinear Adaptive Learning for Electrohydraulic Control Systems,” *Proceedings of the ASME Dynamic Systems and Control Division*, Vol. 5, pp. 83-90, Anaheim, CA, 1998.

APPENDIX

The expression for $\ddot{z}_d(t)$ is given as follows

$$\ddot{z}_d = \frac{1}{\beta_e \zeta} \left(\ddot{f}_d - \beta_e \dot{z} \dot{\xi} - \beta_e z \dot{\xi} + k_3 (\beta_e \zeta \eta_1 - k_3 \eta_z - \eta_f) \right) \quad (73)$$

$$+ \frac{1}{\beta_e \zeta} (\eta_z - k_2 \eta_f - r) - \frac{\dot{\zeta}}{\beta_e \zeta^2} \left(\dot{f}_d - \beta_e z \dot{\xi} + k_3 \eta_z + \eta_f \right)$$

where $\ddot{f}_d(\cdot)$ is given by the following expression

$$\ddot{f}_d = F_d^{(3)} - \beta_e \left(-\frac{\dot{N}_P}{x^2} + \frac{2\dot{x}N_P}{x^3} - \frac{\dot{N}_R}{(L-x)^2} \right) \dot{x} \quad (74)$$

$$+ \frac{2\beta_e \dot{x}^2 N_R}{(L-x)^3} + \beta_e \left(\frac{N_P}{x^2} + \frac{N_R}{(L-x)^2} \right) \ddot{x}$$

$$+ \frac{\beta_e \dot{x}}{m_L} \left(-\frac{A_P}{x^2} + \frac{A_R}{(L-x)^2} \right) (F - N)$$

$$+ \frac{\beta_e}{m_L} \left(\frac{A_P}{x} + \frac{A_R}{L-x} \right) (\dot{F} - \dot{N})$$

$$+ \beta_e \dot{x} \left(-\frac{(C_{ip} + C_{ep})}{x^2} + \frac{C_{ip}}{(L-x)^2} \right) \dot{P}_P$$

$$- \beta_e \dot{x} \left(-\frac{C_{ip}}{x^2} + \frac{C_{ip} + C_{ep}}{(L-x)^2} \right) \dot{P}_R$$

$$+ \beta_e \left(\frac{C_{ip} + C_{ep}}{x} + \frac{C_{ip}}{L-x} \right) \ddot{P}_P$$

$$- \beta_e \left(\frac{C_{ip}}{x} + \frac{C_{ip} + C_{ep}}{L-x} \right) \ddot{P}_R$$

$$+ k_2 (\dot{\eta}_z - k_2 \dot{\eta}_f - \dot{r}) + \frac{1}{m_L} (\dot{\eta}_f - k_1 \dot{r})$$

where $F_d^{(3)}(\cdot)$ is given as follows

$$F_d^{(3)} = m_L \left(x_d^{(5)} + \alpha x_d^{(4)} \right) \quad (75)$$

$$+ \left(\frac{b_L}{m_L} - \alpha \right) \left(\beta_e \left(\frac{\dot{N}_P}{x} - \frac{\dot{x}N_P}{x^2} \right) - k_L \ddot{x} \right)$$

$$+ \left(\frac{b_L}{m_L} - \alpha \right) \left(\beta_e \left(-\frac{\dot{N}_R}{L-x} - \frac{N_R \dot{x}}{(L-x)^2} \right) \right)$$

$$+ \left(\frac{b_L}{m_L} - \alpha \right) (\beta_e (\dot{g}z + g\dot{z}))$$

$$+ \frac{1}{m_L} \left(k_L - b_L \left(\frac{b_L}{m_L} - \alpha \right) \right) (\dot{F} - \dot{N})$$

$$+ \frac{k_1}{m_L} \left(\dot{\eta}_z - k_2 \dot{\eta}_f - \dot{r} - \frac{k_1}{m_L} (\dot{\eta}_f - k_1 \dot{r}) \right)$$

and $\dot{\zeta}(\cdot)$ and $\dot{\xi}(\cdot)$ are given by the following expressions

$$\dot{\zeta} = \frac{d(\nabla_z g)}{dt} z + (\nabla_z g) \dot{z} + \dot{g} \quad (76)$$

$$\dot{\xi} = \frac{d(\nabla_x g)}{dt} \dot{x} + \frac{d(\nabla_{P_P} g)}{dt} \dot{P}_P + \frac{d(\nabla_{P_R} g)}{dt} \dot{P}_R \quad (77)$$

$$(\nabla_x g) \ddot{x} + (\nabla_{P_P} g) \ddot{P}_P + (\nabla_{P_R} g) \ddot{P}_R$$

where

$$\frac{d(\nabla_z g)}{dt} = \frac{k_P \gamma^2 \dot{z} e^{\gamma z} (\beta_1 + 1) + k_P \gamma e^{\gamma z} \dot{\beta}_1}{x (e^{\gamma z} + 1)^2} \quad (78)$$

$$- \frac{k_P \gamma e^{\gamma z} (\beta_1 + 1)}{x^2 (e^{\gamma z} + 1)^3} (\dot{x} (e^{\gamma z} + 1) + 2x\gamma \dot{z} e^{\gamma z})$$

$$+ \frac{k_R \gamma^2 \dot{z} e^{-\gamma z} (\beta_3 + 1) - k_R \gamma e^{-\gamma z} \dot{\beta}_3}{(L-x) (e^{-\gamma z} + 1)^2}$$

$$- \frac{k_R \gamma e^{-\gamma z} (\beta_3 + 1)}{(L-x)^2 (e^{-\gamma z} + 1)^3}$$

$$\cdot (\dot{x} (e^{-\gamma z} + 1) + 2\gamma \dot{z} (L-x) e^{-\gamma z})$$

$$\frac{d(\nabla_x g)}{dt} = \frac{k_R \dot{f}_{sR}}{(L-x)^2} + \frac{2\dot{x}k_R f_{sR}}{(L-x)^3} - \frac{k_P \dot{f}_{sP}}{x^2} + \frac{2\dot{x}k_P f_{sP}}{x^3} \quad (79)$$

$$\frac{d(\nabla_{P_P} g)}{dt} = - \left(\frac{k_P (\dot{x} (e^{\gamma z} + 1) + x\gamma \dot{z} e^{\gamma z})}{2x^2 (e^{\gamma z} + 1)^2} \right) \quad (80)$$

$$\cdot \left(\frac{1}{\sqrt{P_P - P_T}} - \frac{e^{\gamma z}}{\sqrt{P_S - P_P}} \right)$$

$$- \frac{k_P}{2x (e^{\gamma z} + 1)} \left(\frac{\dot{P}_P}{2(P_P - P_T)^{\frac{3}{2}}} \right)$$

$$+ \frac{\gamma \dot{z} e^{\gamma z}}{\sqrt{P_S - P_P}} + \frac{\dot{P}_P e^{\gamma z}}{2(P_S - P_P)^{\frac{3}{2}}}$$

$$\begin{aligned}
\frac{d(\nabla_{P_R} g)}{dt} &= \frac{k_R (\dot{x} (e^{-\gamma z} + 1) + \gamma \dot{z} (L - x) e^{-\gamma z})}{2(L - x)^2 (e^{-\gamma z} + 1)^2} \quad (81) \\
&\quad \left(\frac{1}{\sqrt{P_R - P_T}} - \frac{e^{-\gamma z}}{\sqrt{P_S - P_R}} \right) \\
&\quad - \frac{k_R}{2(L - x) (e^{-\gamma z} + 1)} \left(\frac{\dot{P}_R}{2(P_R - P_T)^{\frac{3}{2}}} \right. \\
&\quad \left. - \frac{\gamma \dot{z} e^{-\gamma z}}{\sqrt{P_S - P_R}} + \frac{\dot{P}_R e^{-\gamma z}}{2(P_S - P_R)^{\frac{3}{2}}} \right)
\end{aligned}$$

and $\ddot{P}_P(\cdot)$, $\ddot{P}_R(\cdot)$ are given in (71) and (72), respectively.